Development of a theoretical model describing sonoporation activity of cells exposed to ultrasound in the presence of contrast agents

Monica M. Forbes
Department of Bioengineering, University of Illinois at Urbana–Champaign, 405 N. Mathews, Urbana, Illinois 61801

William D. O'Brien, Jr.[a),b)]
Department of Electrical and Computer Engineering, University of Illinois at Urbana–Champaign, 405 N. Mathews, Urbana, Illinois 61801

(Received 13 September 2011; revised 24 January 2012; accepted 26 January 2012)

Sonoporation uses ultrasound, with the aid of ultrasound contrast agents (UCAs), to enhance cell permeabilization, thereby allowing delivery of therapeutic compounds noninvasively into specific target cells. The objective of this study was to determine if a computational model describing shear stress on a cell membrane due to microstreaming would successfully reflect sonoporation activity with respect to the peak rarefactional pressure. The theoretical models were compared to the sonoporation results from Chinese hamster ovary cells using Definity® at 0.9, 3.15, and 5.6 MHz and were found to accurately describe the maximum sonoporation activity, the pressure where a decrease in sonoporation activity occurs, and relative differences between maximum activity and the activity after that decrease. Therefore, the model supports the experimental findings that shear stress on cell membranes secondary to oscillating UCAs results in sonoporation.
 [http://dx.doi.org/10.1121/1.3687535]

PACS number(s): 43.35.Ei [CCC] Pages: 2723–2729

I. INTRODUCTION

Sonoporation uses ultrasound (US), with the aid of ultrasound contrast agents (UCAs), to enhance cell permeabilization, thereby allowing delivery of therapeutic compounds noninvasively into specific target cells. The literature suggests that sonoporation is caused by the oscillation of UCAs.[1–4] Two potential physical mechanisms exist for sonoporation as a result of an oscillating UCA: Microstreaming and liquid jets. The literature suggests that liquid jets are the least likely mechanism due to the sporadic nature of liquid jet formation.[2,4–6] Therefore, microstreaming is theorized to be the major mechanism for sonoporation. Microstreaming occurring near a cell can result in shearing motions on the cell membrane, with the potential to cause a biological effect, such as sonoporation.

The studies performed in our laboratory showed a consistent sonoporation response versus peak rarefactional pressure (P_r) for varied UCAs and center frequencies.[1–3] Under our experimental conditions, sonoporation activity (SA) was low at low P_r. As P_r increased, SA increased to a maximum. For some applied frequencies, the maximum SA extended into a plateau as P_r was increased. In all cases, increasing P_r further resulted in a sudden, significant drop in sonoporation. Higher P_r levels, above the inertial cavitation (IC) threshold, resulted in minimal sonoporation activity. The objective of the theoretical development herein is to determine if a model that describes microstreaming-induced shear stress on a cell can describe these sonoporation results.

This shear stress-microstreaming theoretical model was developed by combining several models already in existence. The oscillating UCA was described by the Marmottant model[7] for an UCA located in a sound field. The resulting acoustic streaming velocity gradient near the surface of a bubble was described by Nyborg.[8] Finally, particulars of the sonoporation study, including properties of the medium, exposure duration, and exposure pressures were incorporated into this model. To verify the ability of the shear stress-microstreaming model to predict sonoporation, the results from the model were compared to the experimental results of the SA versus P_r experiments at a variety of exposure conditions.

II. MODELING AN OSCILLATING ULTRASOUND CONTRAST AGENT

The first step in the creation of the shear stress-microstreaming model is to describe the oscillating behavior of an UCA in an ultrasonic field. The Marmottant model for bubble dynamics was chosen because this model incorporates the change in surface tension as the bubble oscillates, in addition to the inclusion of the extra damping due to the presence of the shell and restoring force of the shell.[7] The Marmottant model for bubble dynamics is

$$\rho_L\left(R\ddot{R}+\frac{3}{2}\dot{R}^2\right)=\left[P_0+\frac{2\sigma(R_0)}{R_0}\right]\left(\frac{R}{R_0}\right)^{-3\kappa}\left(1-\frac{3\kappa}{c}\dot{R}\right)-P_0-\frac{2\sigma(R)}{R}-\frac{4\mu\dot{R}}{R}-\frac{4\kappa_s\dot{R}}{R^2}-p_{\mathrm{ac}}(t), \quad (1)$$

[a)]Author to whom correspondence should be addressed. Electronic mail: wdo@illinois.edu
[b)]Also at: Department of Bioengineering, University of Illinois at Urbana-Champaign, 405 N. Mathews, Urbana, Illinois 61801

where R is the time-dependent bubble radius, R_0 is the equilibrium radius of the bubble, ρ_L is the density of the medium, P_0 is the ambient pressure, $\sigma(R)$ is the effective surface tension, κ is the polytropic gas exponent, κ_s is the shell surface viscosity, c is the speed of sound in the medium, μ is the viscosity of the medium, and $p_{ac}(t)$ is the acoustic pressure. The surface tension, $\sigma(R)$ is expressed in terms of the bubble radius,

$$\sigma(R) = \begin{cases} 0 & \text{if } R \le R_{\text{buckling}} \\ \chi\left(\frac{R^2}{R_{buckling}^2} - 1\right) & \text{if } R_{\text{buckling}} \le R \le R_{\text{break-up}}, \\ \sigma_{\text{water}} & \text{if ruptured and } R \ge R_{\text{ruptured}} \end{cases} \quad (2)$$

where χ is the elastic modulus of the elastic regime of the bubble, R_{buckling} is the radius below which the surface of the microbubble buckles, $R_{\text{break-up}}$ is the radius above which the surface shell breaks up, described as $R_{\text{buckling}}(1+\sigma_{\text{water}}/\chi)^{1/2}$, σ_{water} is the surface tension of water, and R_{ruptured} is the radius after rupture, described as $R_{\text{buckling}}(1+\sigma_{\text{water}}/\chi)^{1/2}$.

Solving this equation was accomplished using the ordinary differential equation solver in MATLAB® (The MathWorks, Natick, MA) to find the radius of the UCA versus time. It was assumed that the surrounding medium was a 0.30% 500 kDa Fluorescein isothiocyanate-dextran (FITC-dextran) solution at 20 °C. The driving pulse was described by a 3.15 MHz, 5 cycle cosine pulse, and a P_r of 1 MPa to mimic the pulse used in the sonoporation experiments. A Hanning window was applied to the simulated pulse to make it more representative of an actual transducer pulse. The parameters used in this simulation are listed in Table I.

The first UCA examined was a Definity® microbubble with an equilibrium radius of 1.1 μm. To observe the change in oscillation behavior as P_r changes, a range of P_r values were applied (0.25, 0.75, 1.00, and 1.25 MPa). Figure 1 presents the results from the Marmottant model, the radii (R) of the UCA versus time. As is observed from the results, the negative pressure of the driving waveform causes the UCA to grow and the positive pressure of the driving waveform causes the UCA to shrink. At the lowest P_r value (0.25 MPa) this oscillatory behavior of the UCA is linear, with the same duration for the growth and shrinkage of the UCA. For the higher applied P_r values, the oscillatory behavior of the UCA is nonlinear, with a slower expansion than contraction. For the highest applied P_r values (1 and 1.25 MPa), the contraction of the bubble results in a point of discontinuity. Additionally, the maximum radius of the bubble was greater than 2 times the initial radius. Both of those features indicate that at those two pressures, IC of the UCA was occurring within the single applied pulse.

TABLE I. The parameters and values used to solve the Marmottant model.

Parameter	Value	Description
ρ_L	998 kg/m^3	Fresh water at 20 °C
P_0	101 kPa	Atmospheric pressure
κ	1.07	For perflouropropane
κ_s	32×10^{-9} N for Optison	Optison[1]
	0.5×10^{-9} N for Definity	Definity[2]
c	1480 m/s	For fresh water at 20 °C
μ	0.002 Pa·s	For 0.30% dextran with 500 kDa (Ref. 3)
$P_{ac}(t)$	$P_r \cos(2\pi$ ft)·0.5·[1 − cos(2π ft/cycle)]	
R_{buckling}	R_0	[4]
χ	4 N/m for Optison	Optison[5]
	0.85 N/m for Definity	Definity[2]
R_{breakup}	$R_{\text{buckling}}(1+\sigma_{\text{break-up}}/\chi)^{1/2}$	Ref. 4
$\sigma_{\text{break-up}}$	1 N/m	Ref. 4
R_{ruptured}	$R_{\text{buckling}}(1+\sigma_{\text{water}}/\chi)^{1/2}$	Ref. 4
σ_{water}	0.073 N/m	

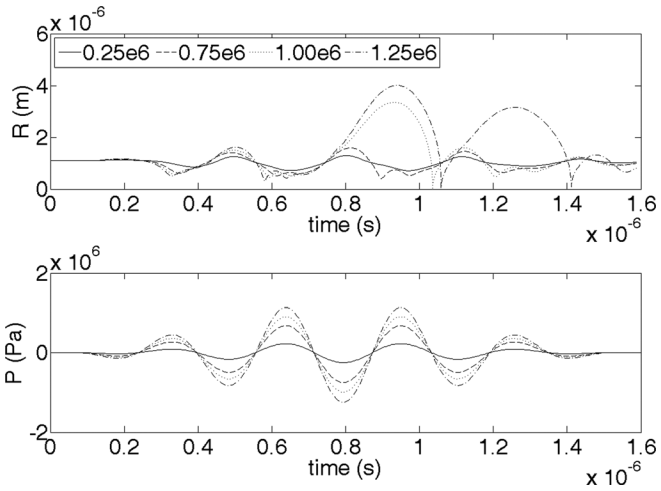

FIG. 1. The radius of a Definity bubble (top) as it changes due to the applied 5 cycle, 3.15 MHz US pulse (bottom) according to the Marmottant model. Each line represents a different P_r, which was varied from 0.25 to 1.25 MPa. R_0 was 1.1 μm.

The maximum radius (R_{max}) was found for P_r values in the range from 0 to 4 MPa. The condition for bubble collapse is a ratio of R_{max}/R_0 greater than 2. When this condition is met, the Marmottant model is no longer valid. The model describes the oscillatory behavior of an UCA, not the IC behavior of a bubble. Figure 2 shows the R_{max}/R_0 for a range of P_r values and the same exposure conditions as for Fig. 1. From these results, the theoretical collapse threshold can be determined for a 1.1 μm Definity microbubble exposed to a 5 cycle, 3.15 MHz pulse in a 0.30% FITC–dextran solution. This threshold, the minimum P_r where R_{max}/R_0 is equal to 2, is 0.816 MPa. The experimental collapse threshold for

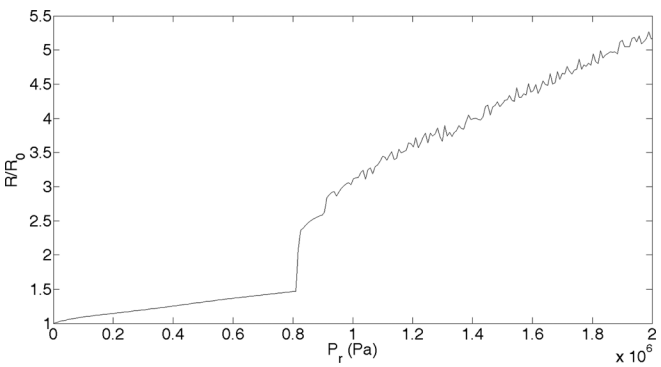

FIG. 2. The ratio of R_{max} to R_0 for a Definity bubble in a 3.15 MHz pulse over a P_r range from 0 to 4 MPa. When the ratio reaches 2, collapse has occurred.

Definity in FITC–dextran exposed to a 5 cycle, 3.15 MHz pulse was 0.95 ± 0.22 MPa.[3] The theoretical collapse threshold is within the error margin of the experimental collapse threshold. The similarity between the theoretical and experimental results supplies confidence in the applicability of the Marmottant model in describing UCA behavior.

III. DESCRIBING THE SHEAR STRESS DUE TO MICROSTREAMING

An oscillating bubble sets up an eddying motion in the surrounding medium that gives rise to microstreaming. The next step of this theoretical development is to determine the acoustic streaming properties of an UCA near a cell. Microstreaming theory finds the shear stress associated with a pulsating bubble near a cell, with knowledge about the initial bubble radius, shear viscosity and density of the medium, frequency of the applied US pulse, and the radial oscillation amplitude of the UCA.[9–13] Shear stress (S) is the final parameter that will be returned from the shear stress-microstreaming model of sonoporation being developed herein.

Rooney[9] describes the shear stress associated with microstreaming as

$$S = \frac{2\pi f \eta \xi_0^2}{a\Delta}, \tag{3}$$

where f is the frequency, η is the shear viscosity of the medium, a is the initial bubble radius, ξ_0 is the radial oscillation amplitude, and Δ is the boundary layer thickness. The boundary layer thickness is defined as

$$\Delta = \left(\frac{\eta}{\rho \pi f}\right)^{1/2}, \tag{4}$$

where ρ is the density of the medium.[10]

An oscillating bubble changes its radius with time, as was verified by the Marmottant model. As a result there are two options for finding the S. The first option is to find the time-varying S as the radius changes with time. This will result in an oscillating S. The second option is to calculate S at one particular time point, specifically when the radius equals R_{max}. At R_{max}, the shear stress will be at its maximum. It is assumed that the maximum shear stress is more important than the oscillating response of the shear stress with respect to impact on the cell membrane. Several articles have shown there is decay in the permeability of the membrane after the ultrasound is turned off. The time scale for a contrast agent, and thus shear stress, to complete one oscillation, is well within the time scales found for cell membrane permeability decay.[4,14] Additionally, the ultimate goal of this theoretical development is to observe how the shear stress changes with P_r. The time-varying S is a complicated result that would add to the complexity of the model without providing significant additional information. As such R_{max} will be used to find the ξ_0, which will then be used to find S.

The time for a fluid flow to develop due to an oscillating UCA must be considered. Several studies have presented observations of streamlines that develop around a vibrating bubble.[9,15] Through visual observation, the smallest streamline traced was approximately 1 and 2 times the circumference of the bubble, respectively. It will be assumed that one circuit of the streamline is sufficient for a fully developed streaming flow to evolve around a bubble that is initially at rest and then excited by US. If we use the more recent value, then the distance the fluid must travel is $2\pi A$ (where A is the initial bubble radius). The limiting tangential fluid velocity (U_L) at the surface of the bubble is given by[10,13]

$$U_L = \frac{2\pi f \xi_0^2}{R_0}. \tag{5}$$

Thus, the time (τ) to complete one circuit of the smallest streamline is

$$\tau = \frac{2\pi R_0}{U_L}. \tag{6}$$

If we assume the radial oscillation amplitude is where the UCA undergoes IC (2 times the initial radius), then ξ_0 is R_0. Thus, τ becomes

$$\tau = \frac{1}{f}. \tag{7}$$

Microstreaming would develop within a single pulse of US at all three frequencies. Therefore, in the development of this model it was assumed that the instant US was turned on microstreaming began.

The next step in developing the shear stress-microstreaming model is to find S [Eq. (3)] at the maximum R_{max}. For this step, the same exposure conditions will be used as in the previous section. A 1.1 μm Definity microbubble is exposed to a 5 cycle, 3.15 MHz pulse in a 0.30% FITC–dextran medium over a range of P_r from 0 to 4 MPa.

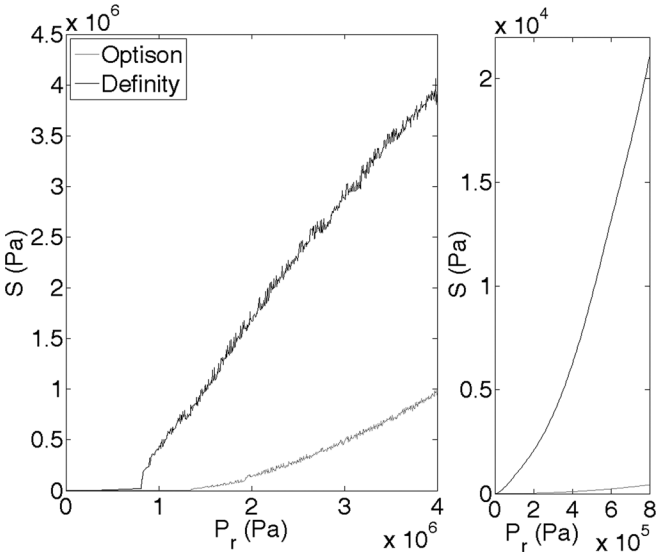

FIG. 3. (Left) Viscous stress (S) from a Definity (black line) and Optison (gray line) bubble oscillating in a 3.15 MHz field, with PD of 5 cycles and PRF of 10 Hz. P_r was varied between 0 and 4 MPa and R_0 was 1.1 μm. (Right) Zoomed in to better appreciate P_r of 0–0.8 MPa.

Figure 3 presents the results of S as a function of P_r. It can be observed that as P_r increases, S increases, just as expected. The same algorithm was applied to a 1.1 μm Optison™ microbubble under the same exposure conditions, with similar results as those for Definity (Fig. 3). Marmottant and Hilgenfeldt[15] demonstrated that unilamellar lipid membranes were ruptured at a shear stress of 10 000 Pa and 180 kHz. From Fig. 3(right), at applied P_r levels of 0–0.8 MPa, S is in the range of 0 to 22 000 Pa for Definity, and 0 to 1300 Pa for Optison. These numbers are of the same order of magnitude as the results by Marmottant and Hilgenfeldt,[15] therefore some measure of confidence exists with this model for shear stress.

IV. APPLYING THE SHEAR STRESS MODEL TO THE SONOPORATION DATA

As the theoretical model currently stands, S increases as P_r increases, indefinitely. The sonoporation results show a drop in sonoporation activity above the collapse threshold. Thus, the next step of this development is to refine the model such that the major features of the sonoporation activity over applied P_r are observed in the theoretical model. The experimental results for sonoporation are presented in Fig. 4 for comparison to the theoretical model.[2,3]

V. INCORPORATION OF A TIME FACTOR IN THE MODEL

Experimentally and theoretically we have shown the collapse threshold of Definity at 5 cycles and 3.15 MHz to be between 0.8 and 0.9 MPa. Because an UCA will collapse when the threshold is reached, a collapsed UCA will exert its viscous stress for a shorter time than those UCAs that do not collapse. Thus, for P_r values greater than the collapse threshold, the shortened time for oscillation will influence the shear stress observed by the cell membrane. Therefore, the model requires a time component to be included.

The first method to incorporate time involved multiplying S by a time factor (t). The time factor is the time duration

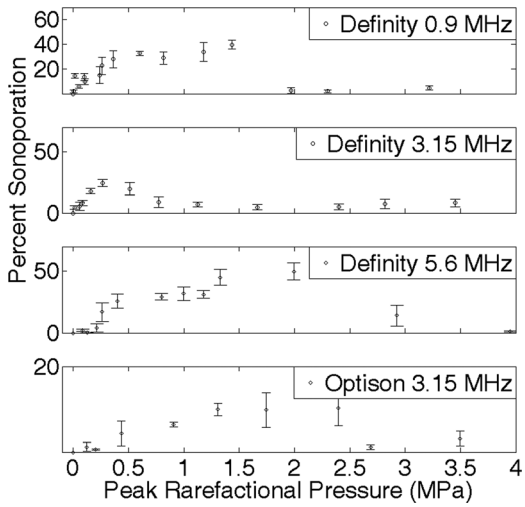

FIG. 4. Percentage of sonoporated cells for exposures with Definity at center frequencies 0.92, 3.15, or 5.6 MHz and Optison at center frequency 3.15 MHz, with 5 cycle PD, 10 Hz PRF, and for 30 s ED (Refs. 7 and 8).

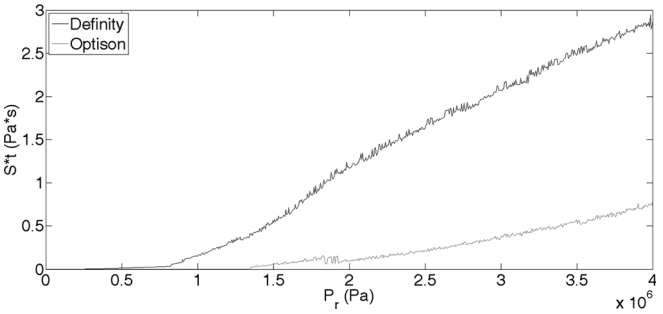

FIG. 5. St from a Definity (black line) and an Optison (gray line) bubble oscillating in a single pulse of 3.15 MHz frequency and PD of 5 cycles. P_r was varied between 0 and 4 MPa and R_0 was 1.1 μm.

an UCA is oscillating due to the applied US pulse. This time factor was chosen with the assumption that the time the cell membrane, in the altered permeability state, is directly proportional to the number of molecules crossing the cell membrane. There are two groups of times to consider: Times for UCAs that do not collapse and times for UCAs that do collapse. The UCAs that do not collapse are present for the entire pulse duration (t_{PD}), thus, in those cases S multiplied by t_{PD} is the time-dependent viscous stress (St_{PD}). For UCA that reach the collapse criterion ($R_{max}/R_0 \geq 2$), the time when the collapse occurs ($t_{collapse}$) is used as the time criterion. Thus, for cases where the UCA collapses, $St_{collapse}$ is the time-dependent stress. This model assumes that there is only one UCA in solution and the moment it collapses, there are no longer any UCAs present.

Figure 5 displays St as a function of P_r for a Definity and an Optison microbubble. The trend for St is the same as for S; as P_r increases St increases. The St result is sigmoid-shaped and smoother than S, with the increase in St occurring at a lower P_r than for S. If the simulated results for Optison in Fig. 5 are compared to the experimental results, more similarity of shape can be seen than for the Definity results. At low P_r values, there is an increase in sonoporation just as there is an increase in St as P_r increases. After reaching a maximum, sonoporation and St drop as P_r increases. However, at this point sonoporation remains low and St rises rapidly as P_r increases. Therefore, further refinement of the theoretical model is needed.

VI. INCORPORATION OF EXPOSURE DURATION INTO THE MODEL

An explanation for the difference between the theoretical and experimental results is the time duration used for the time factor. Currently, the time factor in the model only includes a single pulse. However, experimentally the cells were exposed to the pulsed US conditions for an exposure duration (ED) of 30 s. Thus, the time factor was altered to incorporate the entire ED. For UCAs that collapse, the time factor remains $t_{collapse}$ (it was assumed that the UCA will collapse within the first applied pulse). UCAs that do not collapse are present for the entire ED, thus St_{total} is used for the uncollapsed UCA. t_{total} is defined as the total time the US is turned on during the exposure duration and can be calculated by

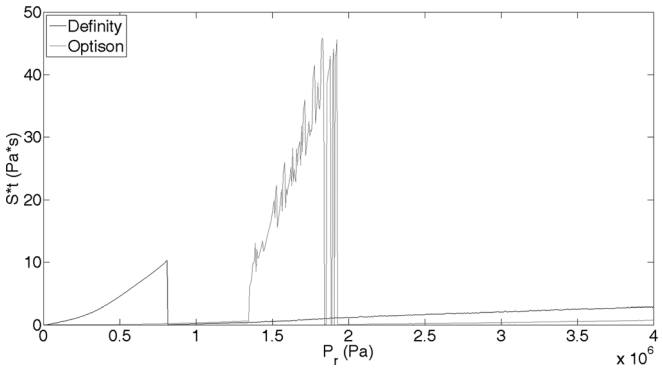

FIG. 6. St_{total} from a Definity (black line) and Optison (gray line) bubble oscillating in a 3.15 MHz field and PD of 5 cycles for an ED of 30 s. P_r was varied between 0 and 4 MPa and R_0 was 1.1 μm.

$$t_{\text{total}} = \begin{cases} \text{PD} \times \text{ED} \times \text{PRF} & \text{noncollapse} \\ t_{\text{collapse}} & \text{collapse} \end{cases}, \tag{8}$$

where PD is the pulse duration and PRF is the pulse repetition frequency (10 Hz). The results from this modified theoretical model are presented in Fig. 6, with Definity and Optison being exposed at the same conditions as mentioned previously.

These refined results present characteristics more similar to the experimental sonoporation data than the results using only a single pulse. Both St_{total} and sonoporation rises as P_r increases; and both reach a maximum followed by a drop off.

Additionally, if the theoretical results between the two contrast agents, Definity and Optison, are compared to the experimental results, similar relationships are observed. The maximum SA for Definity occurred at a P_r of 0.26 MPa. The theoretical model's maximum St_{total} occurs at 0.81 MPa. These P_r values for Definity are in reasonable agreement to each other, giving us confidence in the applicability of the model. The maximum SA for Optison occurred at 2.4 MPa, whereas St_{total} exhibited a maximum at 1.75 MPa. These P_r values, although reasonably close (less than an order of magnitude), are still quite far apart It is noted, however, that the theoretical study for Optison was run at 1.1 μm to be identical to the Definity study. The actual mean diameter of Optison is 2–4.5 μm. If the algorithm is run with a mean radius of 2 μm, the maximum St_{total} occurs at 1.94 MPa (Fig. 7). This result for Optison is closer to the experimental results observed. In both the sonoporation data and St_{total} results, Definity reaches a maximum at a P_r 1–2 MPa lower than that for Optison. This theoretical model shows great potential in describing the microstreaming behavior of a single UCA and how the viscous stress from that streaming correlates to sonoporation of the cell.

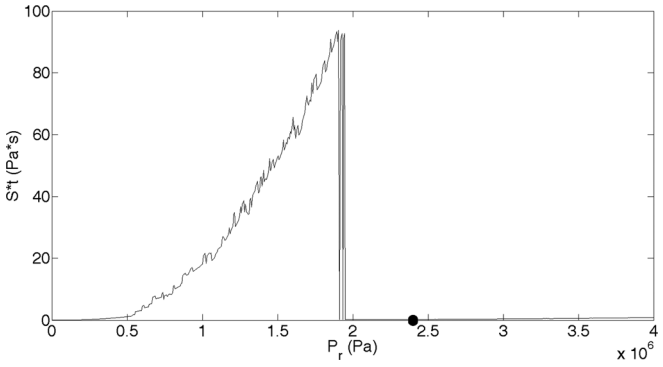

FIG. 7. St_{total} from a Optison bubble oscillating in a 3.15 MHz field and PD of 5 cycles for an ED of 30 s. P_r was varied between 0 and 4 MPa and R_0 was 2 μm. The circle located at 2.4 MPa represents the pressure at which the maximum sonoporation activity occurred under experimental conditions (Ref. 7).

VII. INCORPORATION OF THE DISTRIBUTION OF DEFINITY INTO THE MODEL

Careful study of the theoretical and experimental results reveals one more difference between them. The experimental results displayed a more gradual increase in sonoporation activity as P_r was increased than that observed in the theoretical study. Additionally, the experimental data show more of a plateau when reaching the maximum SA than that observed in the theoretical study. One potential reason for this is that the model currently uses a single UCA at a single radius, whereas a commercial vial of UCAs contains a distribution of sizes. For each radius, this S–t_{total} curve will shift left or right on the P_r axis, depending on the UCA size. If this polydispersion of UCA sizes were incorporated into the model, the theoretical model should more accurately represent the experimental results.

The size distribution of Definity was found using an algorithm developed to measure the radius of the microbubbles on an image. Figure 8 graphically presents the distribution, wherein the radii of Definity varied between 0.025 and 2.23 μm, and the average radius was 0.82 μm. This is similar to the commercial printout that accompanied the Definity vial that stated the mean radius was 0.55–1.65 μm, with 90% of the microbubbles smaller than 10 μm. The distribution of Optison was unable to be measured because Optison was temporarily unavailable for purchase. Therefore, this size modification of the theoretical study was performed only with Definity.

The St_{total} was calculated for every radius found in the Definity distribution. Figure 9a graphically depicts St_{total} for selected single-sized radii sizes using the same exposure

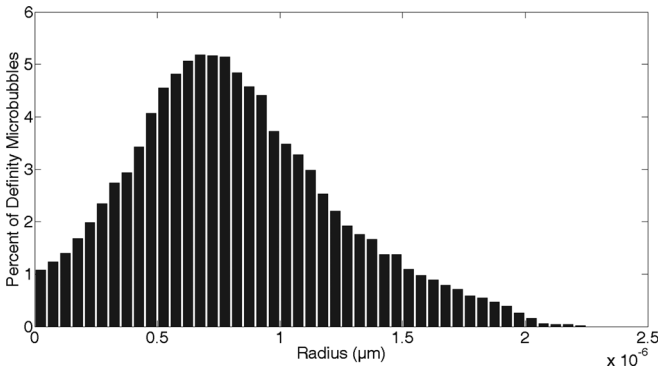

FIG. 8. Size distribution of Definity bubbles immediately following activation.

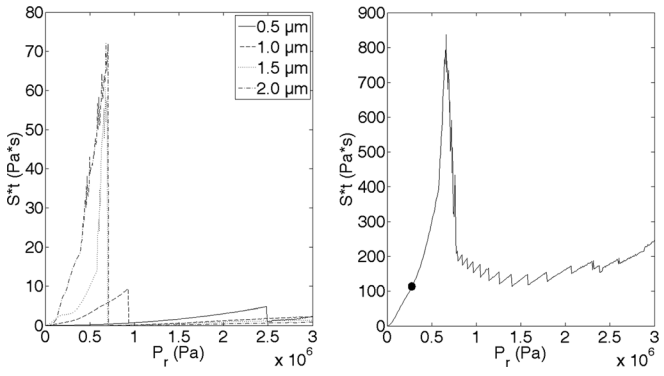

FIG. 9. (Left) St_{total} from Definity oscillating in a 3.15 MHz field and PD of 5 cycles for an ED of 30 s for selected radii sizes (0.5, 1.0, 1.5, and 2.0 μm). P_r was varied between 0 and 3 MPa. (Right) The weighted sum of St_{total} for all radii of Definity at the same exposure conditions. The circle located at 0.26 MPa represents the pressure at which the maximum sonoporation activity occurred under experimental conditions (Ref. 8).

conditions as previously mentioned: 5 Cycle, 3.15 MHz pulse in 0.30% FITC–dextran medium. Figure 9 shows that as the microbubble size increases, the maximum value of St_{total} increases. Also note that as microbubble size increases, the P_r value decreases at which St_{total} is a maximum. It can be observed, therefore, that if obtaining the highest possible value of St_{total} were the goal, then larger radii bubbles at lower P_r in the region of the "spike" would be the ideal setup.

VIII. COMPARISON OF EXPERIMENTAL RESULTS TO THEORETICAL RESULTS

The weighted sum of all the St_{total} was then calculated, using the weights measured from Fig. 8. The resulting weighted sum of St_{total} over all the microbubble radii is plotted in Fig. 9(b). To facilitate the comparison to the experimental data, the 3.15 MHz SA results for Definity in FITC–dextran[3] are presented with the weighted sum of St_{total} in Fig. 10. There are many similarities between the theoretical and experimental sonoporation results. Both results showed a rise in activity to a maximum as P_r was increased. Following the maximum a rapid drop in activity occurs.

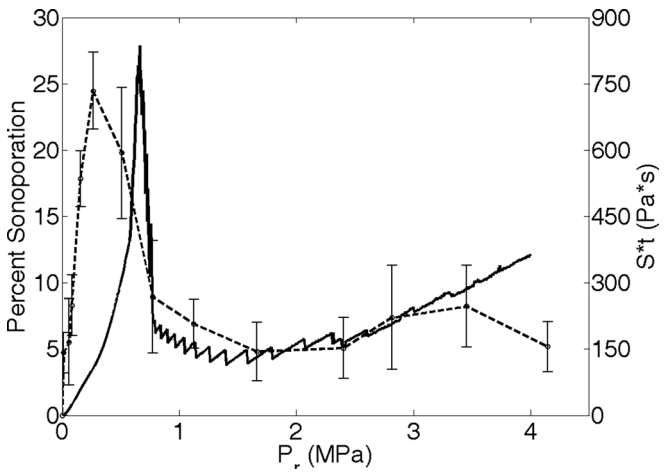

FIG. 10. The weighted sum of St_{total} from Definity oscillating in 3.15 MHz field and PD of 5 cycles for an ED of 30 s and the percentage of sonoporated cells found experimentally at the same exposure conditions (Ref. 8).

Then, as P_r continues to increase the activity remains at a fairly steady lower level. The maximum SA at 3.15 MHz occurred at 0.26 MPa. The maximum St_{total} was at 0.65 MPa. These two results are remarkably close, especially if it is noted that the major portion of the drop-off in SA occurred between 0.51 and 0.77 MPa. The St_{total} maximum occurred in that P_r range. Therefore, the shear stress-microstreaming model is capable of predicting the P_r value at which the maximum St_{total}, and therefore maximum sonoporation occurs. Additionally, the sonoporation activity after the drop off was 20% of the maximum sonoporation activity. The average St_{total} after the drop off was 21% of the maximum St_{total}. These two results again are very similar. The shear stress-microstreaming model is capable of predicting relative quantities of sonoporation activity.

The final test of the shear stress-microstreaming model was to process the model's algorithm with the other two frequencies that were used in sonoporation studies: 0.92 and 5.6 MHz. The SA is presented in Fig. 4. The 0.92 and 5.6 MHz computational model results are presented in Fig. 11. The theoretical results for 0.92 and 5.6 MHz are not as similar to the experimental sonoporation results as that for 3 MHz. For example, the simulated results for 0.92 MHz show a peak occurring at 0.9 MPa, followed by a shallow decrease in St_{total}. The simulated result decrease is much less dramatic than seen in the experimental results. Additionally, following the St_{total} decrease, the simulated model shows the activity rapidly increasing, whereas the SA experimental results remain low. On the other hand, the 5.6 MHz simulated results show both a dramatic drop in St_{total} after the maximum and for P_r values greater than 2 MPa the activity remains low. The 5.6 MHz simulated results, although, show a second peak, between 1.5 and 2 MPa, after the first maximum peak, at 1 MPa. The 5.6 MHz experimental results do not show this second peak, although the sonoporation is elevated until 2.3 MPa. So in both cases the activity is minimal above 2.3 MPa.

Several features are similar between the computational model results and the experimental data and are worth discussing. The P_r values where the maximum sonoporation activity occurred differed among the three frequencies examined, with the 3.15-MHz results occurring at the lowest P_r, 260 kPa, the 0.92 MHz at the next lowest P_r, 1.4 kPa, and the 5.6 MHz at the highest, 2.3 MPa. The model results

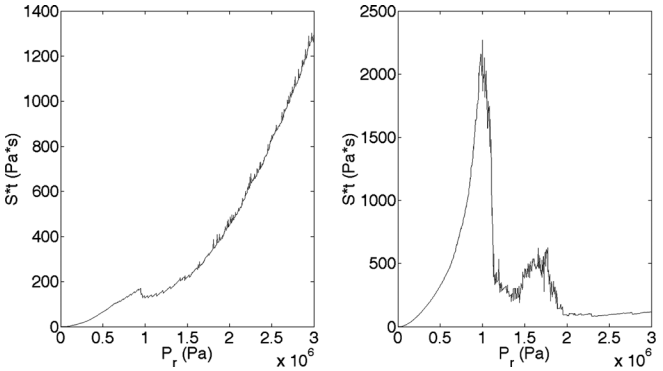

FIG. 11. The weighted sum of St_{total} from Definity oscillating in a (left) 0.92 MHz and a (right) 5.6 MHz field. PD was 5 cycles, ED was 30 s, and P_r was varied between 0 and 3 MPa.

revealed the same pattern, the location of the maximum of the 3.15 MHz results was at the lowest P_r, 0.65 MPa, the 0.92 MHz peak occurred at the next lowest P_r, 0.9 MPa, and the 5.6 MHz peak was at the highest P_r, 1.0 MPa (with a second peak at 1.7 MPa). This similarity in trend further emphasizes the likelihood of a microstreaming mechanism for sonoporation. The microstreaming model was able to reasonably predict the relative locations for the maximum sonoporation activity among different center frequencies.

IX. DISCUSSION

The ability of the computational model to mimic the three major features of the sonoporation activity results (maximum sonoporation activity, drop off in sonoporation activity, and relative differences between maximum activity and the activity after drop off) suggests that shear stress due to microstreaming of an oscillating UCA near a cell is a highly likely a physical mechanism of sonoporation. Additionally, these results verify that the shear stress-microstreaming model can be used to predict the sonoporation activity for different UCAs, radius distribution of the UCAs, exposure medium, ED, and PRF.

The objective of this theoretical study is to determine if a model that describes shear stress on a cell due to microstreaming can describe the sonoporation results regarding the major responses with respect to P_r. The shear stress-microstreaming model has accomplished this objective. The discrepancies found between the model and the experimental results suggest, not unexpectedly, that a more sophisticated model is needed to accurately predict sonoporation activity for various exposure conditions. However, this model as presented revealed great potential and emphasized that even with a crude calculation of shear stress due to microstreaming the major sonoporation responses were revealed.

The shear stress-microstreaming model contained several simplifications that would need to be improved upon for future development. The first was the assumption that the moment the US was turned off (or the UCA collapsed) the microstreaming instantaneously stopped. No consideration for the time to develop the fluid flow to stop was considered. Second, it was assumed that the UCA does not move in and out of the US focus; it is within the focus and in close proximity to the cell for the entire ED. Third, it was assumed that each UCA acted independently of each other, but in nature pressure waves radiated by UCAs in a cloud can accelerate, retard, or even reverse the growth and collapse of other UCAs.[16–18] For this theoretical model, microstreaming flow was described for a single UCA and additive flows from nearby UCAs were not considered. Finally, it was assumed that if an UCA collapsed, it collapsed within the first pulse. Although this is the case in the majority of situations, it has been experimentally observed that collapse can occur in the second and third cycles also.[19] Thus, this simplified model is only a starting point for a more advanced model to describe sonoporation.

The shear stress-microstreaming model presented verifies microstreaming due to oscillating UCAs as the sonoporation mechanism. More development of the model would be required to utilize it as a predictive tool for sonoporation. However, the objective to verify the ability of the shear stress-microstreaming model to predict sonoporation was achieved.

ACKNOWLEDGMENTS

This work was supported in part by an Illinois Distinguished Fellowship for predoctoral students, by NIH Fellowship No. F31EB06634, and by NIH Grant No. R37EB02641. Cell culture facilities were provided by the Imaging Technology Group of the Beckman Institute for Advanced Science and Technology at the University of Illinois at Urbana-Champaign. A special thank you to Darryl Ma for performing the UCA size distribution measurements.

[1]M. M. Forbes, "The role of ultrasound contrast agents in producing sonoporation," Doctor of Philosophy thesis in Bioengineering, Department of Bioengineering, University of Illinois at Urbana–Champaign, IL, 2009.
[2]M. M. Forbes, R. L. Steinberg, and W. D. O'Brien, Jr., "Examination of inertial cavitation of Optison in producing sonoporation of Chinese hamster ovary cells," Ultrasound Med. Biol. **34**, 2009–2018 (2008).
[3]M. M. Forbes, R. L. Steinberg, and W. D. O'Brien, Jr., "Evaluation of the role of Definity® in producing sonoporation of Chinese hamster ovary cells at 0.92, 3.15, and 5.6 MHz," J Ultrasound Med. **30**, 61–69 (2011).
[4]A. van Wamel, K. Kooiman, M. Harteveld, M. Emmer, F. J. ten Cate, M. Versluis, and N. de Jong, "Vibrating microbubbles poking individual cells: Drug transfer into cells via sonoporation," J. Contr. Release **112**, 149–155 (2006).
[5]A. Prosperetti, "A new mechanism for sonoluminescence," J. Acoust. Soc. Am. **101**, 2003–2007 (1997).
[6]E. Brujan, K. Nahen, P. Schmidt, and A. Vogel, "Dynamics of laser-induced cavitation bubbles near elastic boundaries: Influence of the elastic modulus," J. Fluid Mech. **433**, 293–314 (2001).
[7]P. Marmottant, S. van der Meer, M. Emmer, M. Versluis, N. de Jong, S. Hilgenfeldt, and D. Lohse, "A model for large amplitude oscillations of coated bubbles accounting for buckling and rupture," J. Acoust. Soc. Am. **118**, 3499–3505 (2005).
[8]W. L. Nyborg, *Physical Acoustics: Principles and Methods* (Academic, New York, 1964), Vol. 2, Part B.
[9]J. A. Rooney, "Hemolysis near and ultrasonically pulsating gas bubble," Science **169**, 869–871 (1970).
[10]W. T. Coakley and W. L. Nyborg, "Cavitation; dynamics of gas bubbles; applications," in *Ultrasound: Its Applications in Medicine and Biology*, edited by F. J. Fry (Elsevier, Amsterdam, The Netherlands, 1978), Chap 2, pp. 77–159.
[11]S. A. Elder, "Cavitation microstreaming," J. Acoust. Soc. Am. **30**, 54–64 (1959).
[12]NCRP, "Exposure criteria for medical diagnostic ultrasound: II. Criteria based on all known mechanisms," National Council on Radiation Protection and Measurements, Bethesda, MD, 2002, p. 140.
[13]W. L. Nyborg, "Acoustic streaming near a boundary," J. Acoust. Soc. Am. **30**, 329–339 (1958).
[14]C. X. Deng, F. Sieling, H. Pan, and J. Cui, "Ultrasound-induced cell membrane porosity," Ultrasound Med. Biol. **30**, 519–526 (2004).
[15]P. Marmottant and S. Hilgenfeldt, "Controlled vesicle deformation and lysis by single oscillating bubbles," Nature (London) **423**, 153–156 (2003).
[16]M. F. Hamilton, Y. A. Ilinskii, G. D. Meegan, and E. A. Zabolotskaya, "Interaction of bubbles in a cluster near a rigid surface," ARLO **6**, 207–213 (2005).
[17]Y. A. Pishchalnikov, O. A. Sapozhnikov, M. R. Bailey, J. C. Williams, Jr., R. O. Cleveland, T. Colonius, L. A. Crum, A. P. Evan, and J. A. McAteer, "Cavitation bubble cluster activity in the breakage of kidney stones by lithotriptor shockwaves," J. Endourol. **17**, 435–446 (2003).
[18]P. A. Prentice and P. A. Campbell, "Ultrasound-stimulated mutual interaction forces between optically configured micro-bubble pairs," Paper presented at Sixth International Symposium on Therapeutic Ultrasound Conference Proceedings, 2007.
[19]H. G. Flynn and C. C. Church, "Transient pulsations of small gas bubble in water," J. Acoust. Soc. Am. **84**, 985–998 (1988).